Pergamon

J. Mech. Phys. Solids, Vol. 43, No. 6, pp. 829–846, 1995
Elsevier Science Ltd
Printed in Great Britain
0022–5096/95 $9.50 + 0.00

0022–5096(95)00014–3

WRINKLING OF THE OXIDE SCALE ON AN ALUMINUM-CONTAINING ALLOY AT HIGH TEMPERATURES

Z. SUO

Mechanical and Environmental Engineering Department, Materials Department, University of California, Santa Barbara, CA 93106, U.S.A.

(*Received* 20 *October* 1994; *in revised form* 3 *February* 1995)

ABSTRACT

To survive in an oxygen-bearing gas, an alloy grows an oxide scale to cover itself. The scale thickens slowly at a high temperature, until the compressive stress generated by oxidation and cooling causes it to spall off. A widely known model assumes that the scale–alloy interface has unbonded flaws, which allow the scale to buckle under the compression, followed by delamination and cracking. For the scale to buckle under a typical stress, this model requires flaws with radii exceeding ten times the scale thickness. In general, such flaws are too large to be produced during oxidation. This paper proposes a different model. It is commonly observed that wrinkles appear at the high temperature, caused by the oxidation-induced compressive stress. Initially the interface remains bonded, and the alloy conforms to the shape change by creep or diffusion. If the high temperature is maintained long enough, voids will grow on the interface, and the scale will slide, fold and crack. Cooling can intervene at any point; for example, even when the scale only wrinkles without extensive voiding, large thermal stress on the wavy interface may cause the scale to spall off. The initial wrinkling is analyzed as a time-dependent bifurcation by using a variational principle. The base alloy is assumed to conform by metal diffusion along the interface, motivated by the strain energy release due to wrinkling. The results are discussed in connection with experimental observations.

1. INTRODUCTION

Alumina (α-Al_2O_3) is chemically stable and has low self-diffusivities even above 1000°C, making it an excellent oxidation barrier at high temperatures. Many alloys contain aluminum as a component, which preferentially reacts with oxygen in the air to form alumina scales. The scales coat the alloys and thicken slowly at high temperatures, as aluminum and oxygen ions diffuse across the thickness to react with each other. The technology is used in many commercial alloys and in some metal matrix composites.

However, even for these alumina-forming alloys, it is oxidation, rather than creep, that limits lifetime in many applications. The residual stress induced by oxidation and cooling can cause the scales to spall off, exposing the bare alloys to the air. The problem has been extensively investigated; see Stott and Wood (1987), Moon (1989) and Prescott and Graham (1992) for review. An outstanding phenomenon, which has become a point of contact between scientific and commercial studies, is that addition of certain elements to the alloys markedly affects scale integrity. For example, adding less than 1% yttrium prolongs oxide lifetime (e.g. Tien and Pettit, 1972; Whittle and

Stringer, 1980). On the other hand, impurities such as sulfur accelerate spalling (e.g. Smeggil *et al.*, 1986; Sigler, 1988).

Owing to the multiplicity of the rate processes involved, the mechanics of spalling is poorly understood. Even widely used models have basic deficiencies. The rest of this section outlines several elementary considerations that motivate the later sections. Denote the growth stress by σ_G, which is the stress field accumulated when the scale grows at a high temperature, T_G. General understanding of the growth stress has improved over the decades (Stringer, 1970; Evans and Hutchinson, 1994). The stress arises because defects annihilate, molar volumes change due to phase transition, and a new oxide wedges into the existing one. Simultaneously, stress relaxes owing to various creep mechanisms operating in the oxide. In alumina scales, the growth stress is usually compressive, time-dependent, and variable by doping. For example, Quadakkers *et al.* (1989) showed that both aluminum and oxygen diffuse in the scale on an yttrium-free FeCrAl alloy, but only oxygen diffuses in the scale on an yttrium-doped alloy. The former scale wrinkles under the compressive growth stress, but the latter remains flat. It is worth noting that the present understanding is insufficient to calculate the growth stress: it must be measured experimentally. Such measurements for alloys of interest are rare and usually done after cooling to room temperature (e.g. Luthra and Briant, 1986; Diot *et al.*, 1988; Hou and Stringer, 1991). Several general methods are applicable and should improve the understanding of the growth stress in the next few years (Ma and Clarke, 1993; Evans and Hutchinson, 1994).

By contrast, thermal stress is readily predicted. The metal and the oxide both shrink upon cooling from an oxidation temperature T_G to a lower temperature T. Were they unbonded, their strains would differ by

$$\varepsilon_T = \int_{T_G}^{T} (\alpha_m - \alpha_o)\, dT, \tag{1}$$

where α is the thermal expansion coefficient, and the subscripts m and o indicate metal and oxide. Assuming that during cooling the oxide creeps negligibly and remains bonded to the base alloy, this mismatch strain induces a biaxial stress in the plane of the scale, σ_T, given by (Timoshenko and Goodier, 1971)

$$\sigma_T = \frac{E\varepsilon_T}{1-\nu}, \tag{2}$$

where E is Young's modulus and ν is Poisson's ratio of the oxide. Note that the properties of the interface and the alloy, except for its thermal expansion coefficient, do not enter here. Strictly, this formula applies only to a flat scale on an infinitely thick alloy. Taking $E = 400$ GPa and $\nu = 0.25$, and a large strain for a typical scale, $\varepsilon_T = 0.01$, one finds that $\sigma_T = 5$ GPa. The thermal stress is compressive if alumina has a smaller thermal expansion coefficient than the alloy, time-independent if the cooling rate is high enough to neglect oxide creep, and insensitive to doping. (Compressive stress is taken to be positive in this paper.)

The total stress in the scale, σ, is the sum of the two stresses, $\sigma = \sigma_G + \sigma_T$. For a flat scale on a thick alloy, both stresses act biaxially in the plane of the scale; no stress acts on the interface, nor in the alloy. The growth stress may vary through the scale

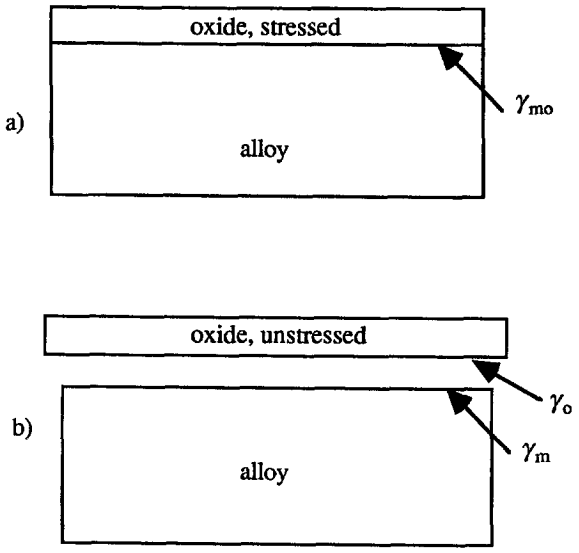

Fig. 1. Free energy model. (a) When the oxide scale is attached to the alloy, the free energy consists of the elastic energy stored in the scale, and the metal–oxide interface energy. (b) When the oxide is off the alloy, the free energy consists of the surface energies of the metal and the oxide. The scale spalls spontaneously if the free energy is reduced, provided a mechanistic process exists.

thickness, but the thermal stress is uniform throughout the scale. Note that, the stress field fluctuates over the length of alumina grain diameter ($\approx 0.1-1$ μm) due to thermal expansion anisotropy of alumina and its growth at the grain boundaries. This fluctuation averages out over the distance of a few grain diameters. For simplicity, unless otherwise stated, we will assume that both σ_G and σ_T are uniform throughout the scale.

Next consider two frequently used models of spalling. The first model compares the free energies before and after debond, see Fig. 1. Denote h as the scale thickness. When the oxide and the metal are bonded, the free energy consists of the elastic energy stored in the scale, $(1-\nu)\sigma^2 h/E$, per unit area, and the metal–oxide interface energy, γ_{mo}. When they detach, the free energy consists of the surface energies of the metal and the oxide, γ_m and γ_o. Thermodynamics require them to debond if the process reduces free energy, namely,

$$(1-\nu)\sigma^2 h/E > \gamma_m + \gamma_o - \gamma_{mo}. \tag{3}$$

According to this criterion, the scale spalls if the stress is high, the scale is thick, the interfacial energy is high, or the free surface energies are low (Evans and Lobb, 1984).

In general, this condition is *necessary*, but *insufficient*. A similar situation nicely illustrates this point. Diamond coating has been successfully spread on a titanium alloy by chemical vapor deposition (Drory and Hutchinson, 1994). The coating, 1 μm thick, is subject to a huge residual compressive stress, $\sigma = 7$ GPa, resulting in 46 J m^{-2} elastic energy per unit area of the coating, which is about an order of magnitude larger than surface energies (< 5 J m^{-2}). Yet the coating sticks on the alloy.

This free energy model is misleading because it does not identify an *evolution path* that links the initial to the final states. The scale indeed becomes thermodynamically unstable, or metastable, when (3) holds. Different paths exist for debond, but they take different stress and time. A path is conceivable, primarily by diffusion, which leads to debond when the stress just satisfies (3), but the time needed may be too long to be of practical interest. Consequently, the issue is not whether to dismiss condition (3), but to study various evolution paths to determine the range of stress and time within which the underlying mechanisms operate.

Figure 2 illustrates a second model which has also long existed in the oxidation literature (e.g. Stringer, 1972). A flat scale cannot debond—no stress acts on the metal–oxide interface. Nor does a small unbonded flaw disturb this mechanical equilibrium. However, a large flaw makes the equilibrium unstable, causing the scale to buckle under the in-plane compressive stress σ. After buckling, stress intensifies on the interface at the buckle front; the flaw spreads if σ is large enough. Evans and Hutchinson (1984), and Hutchinson and Suo (1992) analyzed this buckle–delamination model in terms of fracture mechanics, and found that the flaw spreads approximately like a mode II crack, accompanied by plastic flow in the metal and frictional sliding along the interface. Consequently, delamination resistance can be much larger than surface energies.

Tacitly assumed in these analyses are that buckling is instantaneous, and that

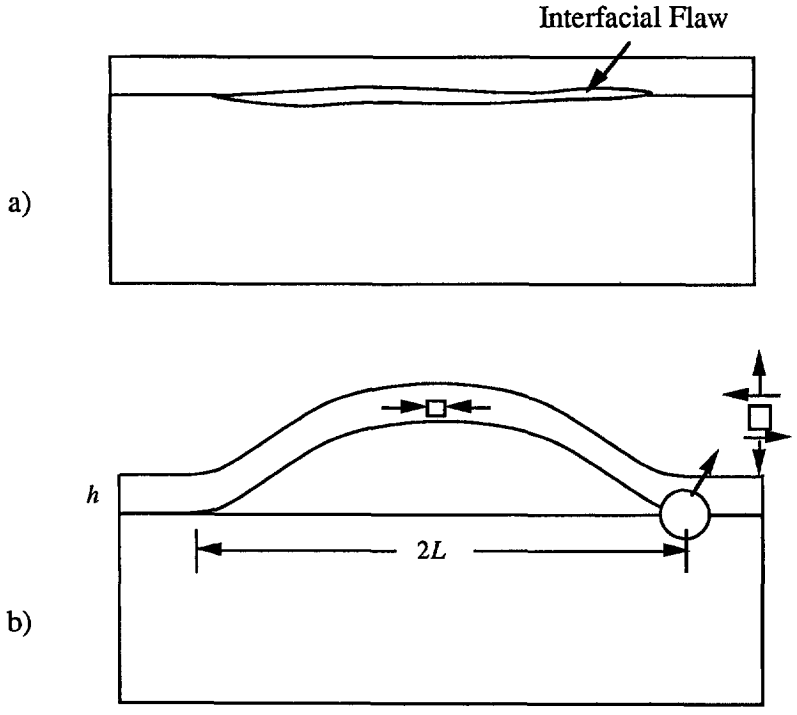

Fig. 2. Buckle–delamination model. (a) Before the scale buckles, no stress acts on the interface to cause a pre-existing flaw to extend. (b) After the scale buckles, stress arises at the front of the flaw.

some kinetic process exists, prior to buckling, to produce the large flaws at a high temperature. Evans *et al.* (1983) questioned this premise: the flaws required for buckling may just be too large to be produced. The critical flaw radius L_c under the compressive stress σ is given by

$$\frac{L_c}{h} = \frac{\pi}{2\sqrt{3}}\left(\frac{E}{\sigma}\right)^{1/2}. \tag{4}$$

Flaws smaller than L_c do not cause buckling, and will not spread since the interface is traction-free. Flaws larger than L_c cause buckling, and will spread if, in addition, the energy release rate exceeds a critical value. The form of the above equation applies to any flaw shape, with the coefficient in the front being close to unity. The value in (4) comes from the classical solution of Euler's buckling column. Taking $\sigma/E = 10^{-2}$, which is a large strain for a typical scale, the critical flaw radius estimated from (4) is $L_c \approx 10h$. Such large cracklike flaws in general cannot be produced by the scale growth process. Both the metal–oxide interface and oxide grain boundaries are active vacancy sinks; a flaw, such as a void, shrinks under surface tension, unless subjected to a tensile stress (Hull and Rimmer, 1959). An explanation is sometimes offered that the probability is high to find *one* large flaw over a large interface area. However, this one flaw can only cause localized spalling, which hardly affects overall oxidation rate.

Given the unusually large flaw size required to start the buckle–delamination process, one is compelled to turn to processes that either produce large flaws, or differ from buckle–delamination. The following section reviews two experimentally observed phenomena, voids and wrinkles, and discusses their roles in spalling.

2. MORPHOLOGICAL EVOLUTION

During oxidation at a high temperature, voids may grow on the metal–oxide interface. In some alloys, voids coalesce to such an extent that the interface remains bonded only at isolated small patches. Speculations abound concerning these voids (see Stott and Wood, 1987). One example illustrates some difficulties in interpreting experimental observations. Sulfur usually exists in alloys as an impurity. Its concentration can be reduced before oxidation by annealing at a high temperature in vacuum or hydrogen (Sigler, 1988; Stasik *et al.*, 1994), or by adding elements like yttrium to tie sulfur in stable sulfides (Smeggil *et al.*, 1986; Sigler, 1993). These experiments demonstrated that voiding reduces markedly when sulfur content drops.

Exactly how sulfur leads to voids remains controversial. Auger spectroscopy has shown that sulfur segregates to metal surfaces (Schmutzler *et al.*, 1992), and possibly to oxide surfaces and metal–oxide interfaces (Smeggil *et al.*, 1986). It is well documented that sulfur-enriched metal surfaces have smaller surface energies, which lower the energy barriers for void nucleation. But what *drives* voids to nucleate and grow to such a large extent? Some answers may be offered, but none of them is of general validity. For example, the stress fluctuation at the alumina grain level, as mentioned before, can give rise to local tension that grows voids—only up to a small size. As a

second example, we note that, in the extreme case when the sulfur-enriched surfaces satisfy

$$\gamma_m + \gamma_o < \gamma_{mo}, \tag{5}$$

namely, when the oxide and metal do not wet each other owing to sulfur segregation, the interface debonds *spontaneously*. Whatever the mechanism, extensive voiding does provide large flaws for buckling. The remaining task is to identify the driving force and estimate the time needed to grow voids, or void clusters, to certain size.

These tantalizing debates aside, it is generally observed that extensive voiding is *not* prerequisite for spalling. More commonly observed are wrinkles, variably called undulations, convolutions and ripples, which appear when the scales grow at a high temperature. Wrinkles are suppressed, within the time of the experiments, by adding yttrium (e.g. Golightly *et al.*, 1976; Tolpygo and Grabke, 1994), or reducing sulfur concentration (e.g. Sigler, 1993, Stasik *et al.*, 1994). These experiments also show high correlation between wrinkling and voiding, and between wrinkling and spalling. Figure 3 sketches snapshots along a morphological evolution path at a fixed high temperature. Micrographs taken from the same alloy showing an entire evolution path are unavailable to this writer. Those cited below were taken from different alloys, but each is believed to be representative of a certain stage of the evolution.

The scale undulates under the compressive growth stress. In the early stage, the alloy deforms and remains bonded with the scale (Fig. 9c in Sigler, 1993). The wrinkles

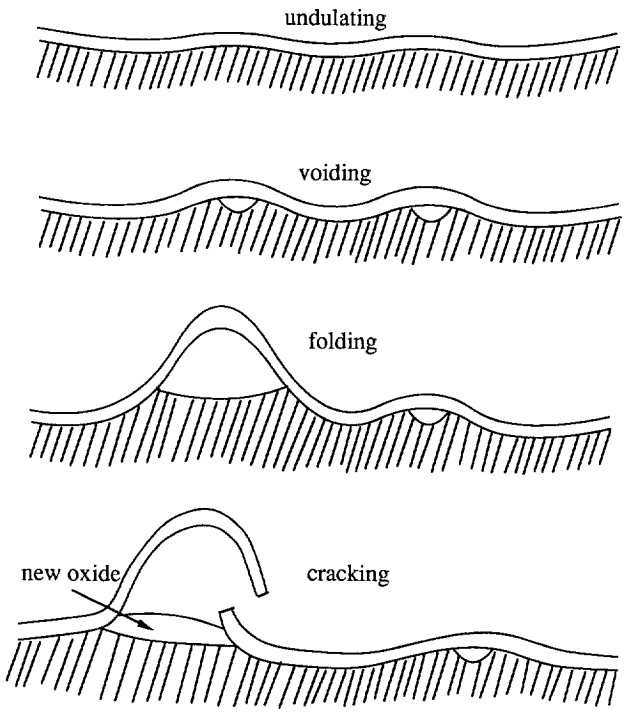

Fig. 3. Sketches of snapshots during isothermal oxidation. Cooling can intervene at any point.

are periodic with a well defined wavelength from a cross-sectional view (Fig. 2a in Hou and Stringer, 1993), and show various patterns from a top view (Fig. 3 in Sigler, 1993; Fig. 2 in Tolpygo and Grabke, 1994). Recall that, before wrinkling, no stress acts on the flat interface or in the base alloy. After wrinkling, stress arises on the wavy interface, motivating the metal to diffuse on the interface and creep in the base alloy. Consequently, wrinkling is a *bifurcation* along the evolution path. Note that the scale wrinkling described here is a different process from the instability of phase boundaries that leads to dendrite growth. The latter does not involve mechanical stresses and results from thermal or chemical diffusion (see Bobeth *et al.*, 1994 and references therein).

As wrinkles amplify, the interfacial stress becomes large enough to drive small voids to grow (Figs 3 and 4 in Tolpygo and Grabke, 1994). Denote $\gamma(\approx 1\ \mathrm{J\ m^{-2}})$ as a representative value of surface energy. To enlarge a void of radius a by diffusion, the necessary tensile stress is estimated by $\sigma = 2\gamma/a$ (Hull and Rimmer, 1959), which gives $\sigma = 20$ MPa for a void of radius $a = 0.1\ \mu$m. Both magnitudes are expected for a wavy interface. Sulfur segregation reduces γ and therefore the stress to grow a void. Consequently, voiding can be a consequence of wrinkling.

This process continues until the periodic wrinkles give way to isolated folds, with large open space between the scale and the alloy (Fig. 3b in Hou and Stringer, 1993). The folds look like domes from a top view. Beneath a fold, the metal surface looks like a smooth shallow crater (Figs 9, 10 in Tien and Pettit, 1972). At this stage, the scale must have slid considerably relative to the alloy to give rise to the large displacement. The inherent viscous interfacial sliding is fast, and is normally limited by the mass transport that accommodates the sliding (Raj and Ashby, 1971). Oxide pegs grown into the base alloy, which have been thought to enhance bonding (Whittle and Stringer, 1980) may also anchor the scale to retard sliding. Note that dome folding is not the most efficient way to reduce the elastic energy. Rather, it is an outcome of a kinetic competition: the diffusion-limited uniform wrinkling and voiding give way to faster sliding to fold fewer, but larger, domes.

The oxide creeps to relax stress, as evident from the observation that some oxide chips remain curved after spalling (Tien and Pettit, 1972). As a fold relaxes the compressive stress in the oxide, more oxide grows in the scale, plating on the oxide grain boundaries. This internal growth, in its turn, amplifies the fold. The scale may crack if stress cannot be sufficiently relieved by creep. The crack allows oxygen to leak in and grow new oxide underneath, pushing the old one to spall off.

A scale can preferentially wrinkle near an alloy grain boundary intersecting the interface. For example, Sigler (1988) showed voids along alloy grain boundaries after the scale had spalled. In an experiment with a hydrogen-annealed FeCrAl, Stasik *et al.* (1994) demonstrated that the scale does not wrinkle over any single grains of the alloy, but folds near an alloy grain boundary. On the other hand, the grain size of high temperature alloys (≈ 50–$500\ \mu$m) is much larger than the scale thickness, and usually larger than the observed wrinkle wavelength. In addition, Tolpygo and Grabke (1994) showed wrinkling on a single crystal FeCrAl alloy. Thus, to focus on wrinkling itself, we will ignore the alloy grain boundaries in this paper, although grain boundaries may play important roles, particularly in alloys that do not wrinkle on grains.

There is nothing unique about the path in Fig. 3. Cooling can punctuate the evolution at any point. Even when the scale only undulates without voiding, large

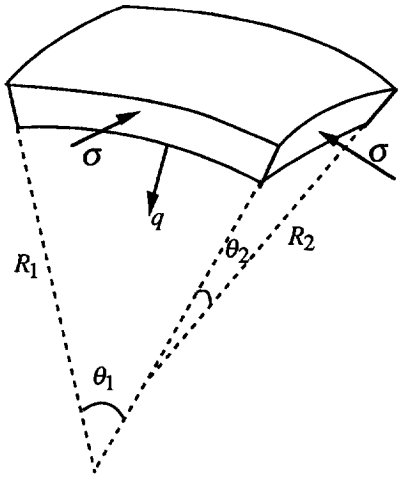

Fig. 4. A free-body diagram for deriving the Laplace–Young formula.

thermal stress on the interface may cause gross spalling. Evans *et al.* (1983) estimated the stress on a wavy interface by considering a scale grown on an alloy cylinder. A slightly more general formula is derived below from a different consideration. Focus on the limiting case when the radius of curvature is large compared to the thickness of the scale. Figure 4 is a free-body diagram, treating the scale as a membrane. Denote R_1 and R_2 as the radii of the principal curvatures; they are positive when the scale is convex toward the air. Neglecting terms of order h/R_1 and h/R_2, the residual stress in the tangential plane of the scale, σ, is unchanged by wrinkling. The stress normal to the interface, q, is determined by equilibrium, resulting in the famous Laplace–Young formula:

$$q = -\left(\frac{1}{R_1} + \frac{1}{R_2}\right)h\sigma. \tag{6}$$

Under the compressive in-plane thermal stress σ, the interfacial stress q is tensile at points convex toward the air, and compressive at points convex toward the base metal. The formula is accurate only in the limit when $h/R_1 \to 0$ and $h/R_2 \to 0$. For the case $\sigma = 5$ GPa and $h/R_1 = h/R_2 = 0.01$, $|q| = 100$ MPa. This large *tensile* stress can drive small interfacial flaws to grow.

In summary, wrinkling gradually reduces the elastic energy: no large flaws are needed to initiate the process. If the high temperature is maintained long enough, voids will grow and the scales will slide, fold and crack. Depending on when cooling intervenes, the scale may or may not spall by the process described by the buckle–delamination model.

3. A VARIATIONAL PRINCIPLE FOR MORPHOLOGICAL EVOLUTION

Although the importance of wrinkles have long been appreciated, to the knowledge of this writer, no models exist that elucidate the role of various parameters. The rest

of the paper will present a model for the initial wrinkling process, when the amplitude is small, the interface remains bonded, and the temperature remains constant (the first stage in Fig. 3). The later stages will be studied elsewhere.

It is interesting to compare the initial wrinkling of an alumina scale to surface roughening of a stressed crystal (Asaro and Tiller, 1972), such as observed on epitaxial films on semiconductor substrates; see Freund and Jonsdottir (1993), Gao (1994), and Yang and Srolovitz (1994) for review. An alumina scale wrinkles when elastic energy reduction due to scale elongation dominates over elastic energy increase due to scale bending, facilitated by creep in the base alloy or diffusion along the alloy–oxide interface. A stressed crystal roughens when elastic energy reduction dominates over surface energy increase, facilitated by diffusion on the crystal surface. In the former, only the in-plane compression causes instability. In the latter, both compression and tension cause instability. It will also become evident that the effect of surface energy is negligible in the former. Of course, the two phenomena bear no resemblance beyond initial bifurcation. Despite these differences, the initial stages of the two phenomena are conceptually analogous. In fact, the following analysis will draw upon the ideas which have emerged in the study of crystal roughening.

As is evident from the description in the last section, wrinkling involves many kinetic processes, ultimately fueled by oxidation. It is undesirable to study them all together in this preliminary attempt. To retain the problem in outline, drastic simplifications are to be made concerning kinetics. It is assumed that, during the time of interest, (a) the scale thickness h remains constant, (b) the growth stress σ_G remains constant, (c) neither scale nor alloy creeps—both deform elastically, and (d) metal ions diffuse on the alloy–scale interface. Assumption (d) retains one kinetic process to allow evolution, while (a), (b) and (c) freeze the other important kinetic processes. These assumptions are justifiable only under limited conditions; for example, bulk diffusion and creep in alloys are likely to be negligible for creep-resistant alloys with large grains. Nonetheless those ignored here are not because they are unimportant; their effects must be studied to fully understand the wrinkling process.

Following our earlier work on stress-driven morphological evolution (Suo and Wang, 1994, Sun *et al.*, 1994), we will formulate the problem in terms of a variational principle. Biot (1970) and others have written on variational principles for irreversible processes. Needleman and Rice (1980) formulated a variational principle for a grain boundary cavitation problem, which they solved by a finite element method. The following presentation focuses on scale wrinkling and is self-contained. We will confine ourselves in two dimensions.

The scale wrinkles without voiding as metal ions diffuse from one part of the interface to another. Two kinematic variables suffice to describe the process: V_n the normal velocity of the interface (volume of atoms per unit time added per unit area of the interface), and J the atomic flux in the interface (number of atoms per unit time crossing per unit length on the interface). Mass conservation requires that the flux divergence be related to the velocity as

$$\frac{\partial J}{\partial s} + \frac{V_n}{\Omega} = 0, \tag{7}$$

where s is the length measured along the interface, and Ω the volume of each lattice site.

The system is in mechanical equilibrium and, at a given time, the stress field is determined by the static elasticity theory. The system is also in thermal equilibrium with a uniform temperature. Within the assumed kinetics, the system is not in thermodynamic equilibrium only because metal ions diffuse on the interface. Let Φ be the free energy of the system, consisting of elastic energy stored in both the scale and the alloy (after wrinkling), and the surface energy of the oxide surface and oxide–metal interface. Let the time rate of the free energy be $\dot{\Phi}$. Thermodynamics require that $\dot{\Phi} = 0$ when the system is in equilibrium, and $\dot{\Phi} < 0$ when the system is undergoing an irreversible process to approach the equilibrium.

This global energetic description, viewing the system as a whole, also has a local counterpart in terms of thermodynamic forces. Define the diffusion driving force per atom, F, as the free energy reduction associated with an atom moving unit distance, namely

$$\dot{\Phi} + \int FJ \, \mathrm{d}s = 0. \tag{8}$$

The integration extends over the interface. In defining the driving force by (8), flux and velocity can be any *virtual* distributions that obey mass conservation (7). The virtual flux and the driving force need not satisfy any kinetic relation. As shown before (Suo and Wang, 1994), this formulation bypasses, but is equivalent to, the one involving chemical potential as an intermediate variable. It will directly lead to a variational principle.

The atomic mobility on the metal–oxide interface is described in the usual way. The *actual* flux linearly depends on the driving force:

$$J = MF. \tag{9}$$

The atomic mobility, M, is related to the interfacial diffusivity by the Einstein relation, $M = D_i \delta_i / \Omega k T$. Here D_i is the interfacial diffusivity, δ_i the effective thickness participating in the diffusion process, k Boltzmann's constant, and T the absolute temperature. Only metal ions are assumed to diffuse along the interface and, among all the elements in the alloy, the slowest diffusing element limits the evolution rate.

We identify a variational principle for this nonequilibrium thermodynamic process. Of all the virtual fluxes that obey mass conservation (7), the actual flux minimizes the functional

$$\Pi = \dot{\Phi} + \int \frac{J^2}{2M} \mathrm{d}s. \tag{10}$$

At a given time, Π is a functional of the virtual flux J—that is, any arbitrary distribution J gives a value of Π. The calculation of Π involves solving an incremental elasticity problem with matter inserted along the interface at velocity V_n as determined from J by (7). The actual flux is selected to minimize Π. Once the flux is determined, the associated velocity V_n updates the geometry for a small time increment, and the procedure repeats itself with the new geometry. Thus, the variational principle governs J and V_n at any given time, and evolution is traced by time stepping.

This variational principle is equivalent to (8) and (9), as proved below. Let J be

the actual flux and Q a virtual flux, so that $J+Q$ is also a virtual flux. The free energy Φ is independent of the kinematic variables, and its rate is linear in the virtual flux, i.e.

$$\dot{\Phi}(J+Q)-\dot{\Phi}(J)=\dot{\Phi}(Q). \tag{11}$$

Consequently, the difference in Π is given by

$$\Pi(J+Q)-\Pi(J)=\dot{\Phi}(Q)+\int\frac{J}{M}Q\,\mathrm{d}s+\int\frac{Q^2}{2M}\mathrm{d}s. \tag{12}$$

The actual flux J satisfies the kinetic relation (9), so that $J/M=F$ in the above. Because (8) holds for any virtual flux, and in particular for Q, the above equation reduces to

$$\Pi(J+Q)-\Pi(J)=\int\frac{Q^2}{2M}\mathrm{d}s, \tag{13}$$

which is always nonnegative. Thus the proof: $\Pi(J+Q)\geqslant\Pi(J)$ for any virtual flux Q.

4. LINEAR BIFURCATION ANALYSIS

A flat scale is in equilibrium—no stress acts on the interface or in the alloy. Yet this equilibrium is unstable under the compressive stress σ_G in the scale. Figure 5 shows the geometry of a wavy scale, with the x-axis lying on the initially flat interface. Assume that the scale bifurcates into a sinusoidal shape

$$y(x,t)=A(t)\sin(\pi x/L), \tag{14}$$

with amplitude $2A$ and wavelength $2L$. In the following analysis, the wavelength is fixed, and the system is described with only one degree-of-freedom, the amplitude A. The analysis will determine the amplitude as a function of time, $A(t)$.

We will only carry out a linear bifurcation analysis, where the amplitude is much smaller than the wavelength, $A/L\ll 1$. All the results will be retained to the leading order in A. The variational principle applies to one half of the wavelength, $0<x<L$. Two geometric relations are readily obtained. The radius of curvature, R, is given by

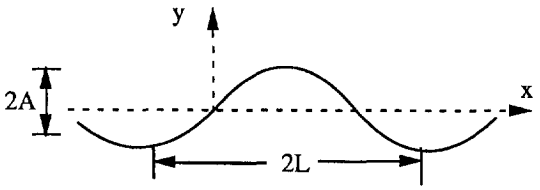

Fig. 5. Geometry of a wrinkling scale.

$$\frac{1}{R} = -\frac{\partial^2 y}{\partial x^2} = A\left(\frac{\pi}{L}\right)^2 \sin\left(\frac{\pi x}{L}\right). \tag{15}$$

Within half a wavelength, the scale elongates by

$$\Delta = \int_0^L \sqrt{1+(\partial y/\partial x)^2}\,\mathrm{d}x - L = \frac{\pi^2}{4} A^2/L. \tag{16}$$

When compressed to wrinkle, the scale changes elastic energy in two ways: the bending increases the energy, but the elongation reduces the energy. The elementary beam theory shows that

$$\Phi = \frac{Eh^3}{24}\int_0^L \frac{\mathrm{d}x}{R^2} - \sigma_G h\Delta = \frac{h\pi^2}{4L}\left[\frac{\pi^2 E}{12}\left(\frac{h}{L}\right)^2 - \sigma_G\right]A^2. \tag{17}$$

Equations (15) and (16) have been used to complete the calculation. The analysis focuses on isothermal oxidation, when only the growth stress σ_G is present in the scale.

The elastic energy in the alloy and surface energies are ignored, as justified below. Combining (6) and (15), the interfacial stress is

$$q(x) = \sigma_G h A\left(\frac{\pi}{L}\right)^2 \sin\left(\frac{\pi x}{L}\right).$$

As expected, this stress is much smaller than the in-plane stress σ_G for a small wave amplitude. The sinusoidal traction induces an elastic field in the alloy, which is approximated by a semi-infinite solid subject to a sinusoidal surface traction. The displacement on the interface takes the form $u(x) \approx Lq(x)/E$ (Timoshenko and Goodier, 1971). The numerical coefficient has been ignored, as it will be in all the estimates in this paragraph. The elastic energy stored in the alloy equals the work done by the traction:

$$W = \frac{1}{2}\int_0^L uq\,\mathrm{d}x \approx \frac{\sigma_G^2}{E}\left(\frac{hA}{L}\right)^2.$$

Its magnitude should be compared with the energy reduction due to scale elongation, the second term in (17). The ratio is $(\sigma_G/E)(h/L)$, which is small. Next consider the contribution of surface energy. Due to wrinkling, the surface energy increases by $\gamma\Delta$, where γ is a representative value of the surface energy (≈ 1 J m^{-2}). The ratio of this increase over the second term in (17) is $\gamma/(\sigma_G h)$, which is small for stress in the GPa and thickness in the micrometer range.

The scale wrinkles only if the process reduces the free energy. According to (17), the free energy changes sign at a critical wavelength L_c given by

$$\frac{L_c}{h} = \frac{\pi}{2\sqrt{3}}\left(\frac{E}{\sigma_G}\right)^{1/2}. \tag{18}$$

When $L < L_c$, the bending energy increase dominates, and the scale flattens. When

$L > L_c$, the elongation energy reduction dominates, and the scale wrinkles. As expected, formula (18) is identical to (4), but only the growth stress now appears.

The profile (14) with $A/L \ll 1$ yields the velocity

$$V_n = \dot{A} \sin(\pi x/L). \tag{19}$$

Integration of (7) gives the flux

$$J = \frac{L\dot{A}}{\pi\Omega} \cos(\pi x/L). \tag{20}$$

The integration constant vanishes because $J = 0$ at $x = L/2$, as dictated by the symmetry.

Inserting (17) and (20) into (10) gives

$$\Pi(\dot{A}) = \frac{h\pi^2}{2L}\left[\frac{\pi^2 E}{12}\left(\frac{h}{L}\right)^2 - \sigma_G\right] A\dot{A} + \frac{L^3}{4\pi^2 M\Omega^2}\dot{A}^2. \tag{21}$$

For this one degree-of-freedom system, Π is a function of only one variable, $\dot{A}$, and is minimized by setting $\mathrm{d}\Pi/\mathrm{d}\dot{A} = 0$, resulting in a linear ordinary differential equation

$$\dot{A} = A/\tau, \tag{22}$$

with the characteristic time

$$\tau = \frac{L^4}{\pi^4 M\Omega^2 Eh}\left[\frac{\sigma_G}{E} - \frac{\pi^2}{12}\left(\frac{h}{L}\right)^2\right]^{-1}. \tag{23}$$

The solution to (22) is

$$A(t) = A_0 \exp(t/\tau), \tag{24}$$

where A_0 is the amplitude at the time $t = 0$. The implications of these results are discussed in the next section.

5. WAVELENGTH SELECTION AND CHARACTERISTIC TIME

In the beginning, the scale is not perfectly flat. The imperfection contains infinitely many sinusoidal components, each having its own wavelength. Equation (24) shows that a component either amplifies or decays exponentially with time, depending on whether τ is positive or negative. Figure 6 sketches the characteristic time τ as a function of the wavelength L. The characteristic time changes sign at the critical wavelength, L_c, given by (18). For a smaller wavelength, $L < L_c$, the characteristic time $\tau < 0$; the energy increase due to bending dominates, and the component decays with time. For a larger wavelength, $L > L_c$, the characteristic time $\tau > 0$; the energy reduction due to elongation dominates, and the component amplifies with time.

Why does the wrinkle select a particular wavelength? Imagine that all the sinusoidal components with wavelengths exceeding L_c are striving to amplify. The component having the smallest τ amplifies most rapidly, and is therefore expected to win the race.

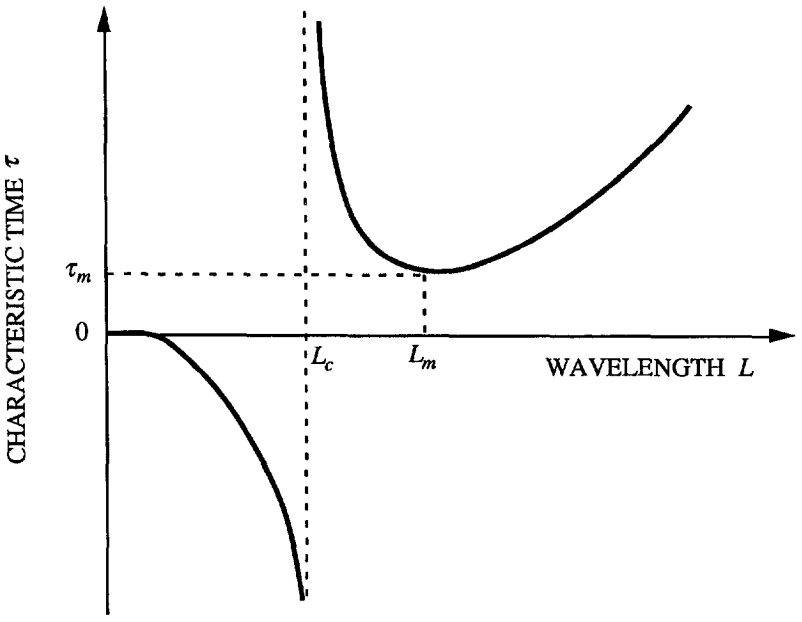

Fig. 6. When the wrinkle amplitude is small compared to the wavelength, the amplitude evolves exponentially with a characteristic time that depends on the wavelength. Sketched here are the important features of this dependence.

The characteristic time τ, in turn, varies with the wavelength L. The trends in Fig. 6 are dictated by robust features of the energetics and the assumed kinetics. For a component with wavelength just exceeding L_c the driving force is small, and wrinkling takes a long time. For a component with very long wavelength, atoms diffuse over long distances, and wrinkling also takes a long time. Consequently, a wavelength L_m exists that minimizes the characteristic time τ. According to (23), this wavelength is given by

$$\frac{L_m}{h} = \frac{\pi}{2\sqrt{2}}\left(\frac{E}{\sigma_G}\right)^{1/2}. \tag{25}$$

Within the present model, the wrinkles most likely select this wavelength. Observe that L_m is not too much larger than L_c in (18).

According to (25), a growth stress in the GPa range makes the wavelength exceed 20 times the scale thickness. (L is only a half of the wavelength.) This prediction is larger than experimentally observed wavelengths, which are usually a few times the scale thickness (e.g. Hou and Stringer, 1993; Sigler, 1993; Tolpygo and Grabke, 1994). The apparent discrepancy can be understood as follows. We have assumed in the analysis that the scale starts wrinkling at a fixed thickness h. In comparing the experiments, we have arbitrarily identified h with the thickness at which the micrographs happened to be taken. In reality, a scale may wrinkle at a much earlier time. A short wave, having developed when the scale is thin, either decays as the scale

Table 1. *Behaviors of differently treated FeCrAl alloys*

Treatment	Wrinkling	Voiding	Spalling	References
Untreated	Yes	Yes	Yes	a,b,c
Annealed in H_2 or vacuum	No†	No	No	a,b
Doped with yttrium	No	No	No	a,b,c
Doped with titanium	Yes	No	No	a,b

a, Sigler (1993). b, Stasik *et al.* (1994). c, Tolpygo and Grabke (1994).
†The scale is planar over the grains of the alloy, but wrinkles near grain boundaries of the alloy.

thickens, or is preserved if the stress in the scale is partially relieved by oxide creep. For example, Quadakkers *et al.* (1989) and Tolpygo and Grabke (1994) showed that the wavelength remains unchanged after some early stage of oxidation. Our present model does not give any prediction about when the wavelength is selected. To do so would require that the model also include the kinetics of oxide growth and stress generation.

According to (23), the minimum characteristic time associated with the wavelength L_m is

$$\tau_m = \frac{3h^3E^2}{64M\Omega^2\sigma_G^3}. \tag{26}$$

It has strong dependence on scale thickness and growth stress. They are readily understood as follows. A thick scale wrinkles at a large wavelength, transfers matter over a long distance, and therefore takes a long time. A large growth stress not only increases the diffusion driving force, but also selects a short wavelength. The sensitive dependence of the wrinkling rate on scale thickness suggests that, if an additional layer is coated over the alumina scale, such as a zirconia thermal barrier, wrinkling will become difficult because of the large bending energy increase. It is conceivable that strategies other than a thermal barrier coating can also achieve this effect.

The present result shows that the growth stress has a nonlinear effect on wrinkling rate. One possible effect of yttrium is that it may reduce the growth stress (Golightly *et al.*, 1976, Tolpygo and Grabke, 1994). However, direct stress measurement is unavailable to prove this effect. Table 1 lists behaviors of FeCrAl alloys subject to different treatment prior to oxidation tests. The compositions of major alloy elements are similar, Fe-20Cr-5Al wt%. The scales are about 1 μm thick after oxidizing at 1000°C for 100 h. (Exact compositions and testing conditions vary among the studies; the numbers quoted here are approximate.) An alloy annealed in vacuum or hydrogen has low sulfur concentration. Its qualitative behavior is identical to yttrium-doped alloys in all three categories. Since both scales are flat, the growth stress could be measured without ambiguity. The results, in conjunction with the existing observations, would help to clarify various effects that yttrium and sulfur have been implicated.

6. CONCLUDING REMARKS

Spalling is a nonequilibrium thermodynamic phenomenon involving multiple kinetics, fueled ultimately by oxidizing aluminum. It is important to examine the entire morphological evolution path during isothermal oxidation. Ample micrographs now exist that give revealing snapshots of many alloys under many testing conditions, but little is certain about the entire evolution path of any particular ones. The morphological evolution following wrinkling is reviewed in this article. Wrinkles induce interfacial stress and cause voiding. In later stages the scale slides, folds and cracks. It is remarkable that little attention has been paid to the effect of alloy creep and interfacial diffusion, given that wrinkles and voids are so commonly reported.

This paper carries out a linear bifurcation analysis when wrinkles just start. The model as it stands now, although incomplete, is suggestive. It confirms the importance of the growth stress and assigns a new role to thermal barrier coatings. Within the kinetics assumed in this paper, wrinkling is unavoidable, but the characteristic time is sensitive to growth stress, scale thickness, and interfacial diffusivity. Doping is important to the extent that it affects the preceding quantities. Considering the multiplicity of kinetic processes, the various doping effects can result simply because the evolution path is altered by accelerating one process or decelerating another. It is hoped that a study of competing kinetics will soon succeed in revealing diverse evolution paths.

ACKNOWLEDGEMENTS

The writer did the work during a sabbatical leave at the Max-Planck Institute at Stuttgart, Germany, sponsored by the Alexander von Humboldt Foundation through a Research Fellowship, and by the Max-Planck Institute at Stuttgart. The hospitalities of Professors M. Ruhle and E. Arzt of the Institute are gratefully acknowledged. The writer thanks Professor D. R. Clarke at UCSB and participants of Professor Ruhle's group on high temperature oxidation for stimulating discussions. The written comments by Dr P. Y. Hou, Professors H. E. Evans, G. H. Meier and F. H. Stott on an earlier version of the manuscript have educated the writer. The work was supported by the Advanced Research Projects Agency through the University Research Initiative under the Office of Naval Research contract N-0014-92-J-1808, and by the National Science Foundation through a Young Investigator Award MSS-9258115.

REFERENCES

Asaro, R. J. and Tiller, W. A. (1972) Interface morphology development during stress corrosion cracking: Part I. Via surface diffusion. *Metall. Trans.* **3,** 1789–1796.

Biot, M. A. (1970) *Variational Principles in Heat Transfer.* Oxford University Press, Oxford.

Bobeth, M., Pompe, W., Rockstroth, M. and Schumann, E. (1994) Morphological instability of a planar oxide–alloy interface for inward oxide growth. *Acta. Metall. Mater.* **42,** 579–588.

Diot, C., Chouquet, P. and Mevrel, R. (1988) Simultaneous determination of residual stresses in a thin alumina layer grown by oxidation on a NiCoCrAlY alloy and in this alloy. *Int. Conf. Residual Stresses* (ICRS-2) (ed. G. Beck, S. Denis and A. Simon), pp. 273–278. Elsevier Applied Science, London.

Drory, M. D. and Hutchinson, J. W. (1994) Diamond coating of titanium alloys. *Science* **263,** 1753–1755.

Evans, A. G., Crumley, G. B. and Demaray, R. E. (1983) On the mechanical behavior of brittle coatings and layers. *Oxid. Met.* **20,** 193–216.

Evans, A. G. and Hutchinson, J. W. (1984) On the mechanics of delamination and spalling in compressed films. *Int. J. Solids Structures* **20,** 455–466.

Evans, A. G. and Hutchinson, J. W. (1994) The thermomechanical integrity of thin films and multilayers. *Acta. Metall. Meter.* (in press).

Evans, H. E. and Lobb, R. C. (1984) Conditions for the initiation of oxide-scale cracking and spallation. *Corrosion Sci.* **24,** 209–222.

Freund, L. B. and Jonsdottir, F. (1993) Instability of a biaxially stressed thin film on a substrate due to material diffusion over its free surface. *J. Mech. Phys. Solids* **41,** 1245–1264.

Gao, H. (1994) Some general properties of stress-driven surface evolution in a heteroepitaxial thin film structure. *J. Mech. Phys. Solids* **42,** 741–772.

Golightly, F. A., Stott, F. J. and Wood, G. C. (1976) The influence of yttrium additions on the oxide-scale adhesion to an iron–chromium–aluminum alloy. *Oxid. Met.* **10,** 163–187.

Hou, P. Y. and Stringer, J. (1991) Room temperature strains in Cr_2O_3 scales formed at elevated temperatures on Ni–25wt%Cr and Y- and Al-doped Ni–25wt%Cr. *Acta Metall Mater.* **39,** 841–849.

Hou, P. Y. and Stringer, J. (1993) Effect of surface-applied reactive elements on early stage oxidation of Fe–18Cr–5Al and Fe–18Cr–5Al-1HF alloys. *J. De Physique* **3,** 231–240.

Hull, D. and Rimmer, D. E. (1959) The growth of grain-boundary voids under stress. *Phil. Mag.* **4,** 673–687.

Hutchinson, J. W. and Suo, Z. (1992) Mixed-mode cracking in layered materials. *Adv. Appl. Mech.* **29,** 63–191.

Luthra, K. L. and Briant, C. L. (1986) Mechanism of adhesion of alumina on MCrAlY alloys. *Oxid. Met.* **26,** 397–416.

Ma, Q. and Clarke, D. R. (1993) Stress measurement in single-crystal and polycrystalline ceramics using their optical fluorescence. *J. Am. Ceram. Soc.* **76,** 1433–1440.

Moon, D. P. (1989) Role of reactive elements in alloy protection. *Mater. Sci. Tech.* **5,** 754–764.

Needleman, A. and Rice, J. R. (1980) Plastic creep flow effects in the diffusive cavitation of grain boundaries. *Acta Metall.* **28,** 1315–1332.

Prescott, R. and Graham, M. J. (1992) The formation of aluminum oxide scales on high-temperature alloys. *Oxid. Met.* **38,** 233–254.

Quadakkers, W. J., Holzbrecher, H., Briefs, K. G. and Beske, H. (1989) Difference in growth mechanisms of oxide scales formed on ODS and conventional wrought alloys. *Oxid. Met.* **32,** 67–88.

Raj, R. and Ashby, M. F. (1971) On grain boundary sliding and diffusional creep. *Metall. Trans.* **2,** 1113–1127.

Schmutzler, H. J., Viefhaus, H. and Grabke, H. J. (1992) The influence of oxide/metal interface composition on the adherence of oxide layers on metal substrates. *Surface Interface Anal.* **18,** 581–584.

Sigler, D. R. (1988) The influence of sulfur on adherence of Al_2O_3 grown on Fe–Cr–Al alloys. *Oxid. Met.* **29,** 23–43.

Sigler, D. R. (1993) Adherence behavior of oxide grown in air and synthetic exhaust gas on Fe–Cr–Al alloys containing strong sulfide-forming elements: Ca, Mg, Y, Ce, La, Ti, and Zr. *Oxide. Met.* **40,** 555–583.

Smeggil, J. G., Funkenbusch, A. W. and Bornstein, N. S. (1986) A relationship between indigenous impurity elements and protective oxide scale adherence characteristics. *Metall. Trans.* **17A,** 923–932.

Stasik, M. C., Pettit, F. S., Meier, G. H., Ashary, A. and Smialek, J. L. (1994) Effects of reactive element additions and sulfur removal on the oxidation behavior of FeCrAl alloys. *Scripta Metall. Mater.* **31,** 1645–1650.

Stott, F. H. and Wood, G. H. (1987) Growth and adhesion of oxide scale of Al_2O_3 forming alloys and coatings. *Mater. Sci. Engng* **87,** 267–274.

Stringer, J. (1970) Stress generation and relief in growing oxide films. *J. Corrosion Sci.* **10,** 513–543.
Stringer, J. (1972) Stress generation and adhesion in growing oxide scales. *Werkstoffe und Korrosion* **9,** 747–55.
Sun, B., Suo, Z. and Evans, A. G. (1994) Emergence of crack by mass transport in elastic crystals stressed at high temperatures. *J. Mech. Phys. Solids* **42,** 1653–1677.
Suo, Z. and Wang, W. (1994) Diffusive void bifurcation in stressed solid. *J. Appl. Phys.* **76,** 3410–3421.
Tien, J. K. and Pettit, F. S. (1972) Mechanism of oxide adherence on Fe–25Cr–4Al (Y or Sc) alloys. *Metall. Trans.* **3,** 1587–1599.
Timoshenko, S. P. and Goodier, J. N. (1971) *Theory of Elasticity*. McGraw-Hill, New York.
Tolpygo, V. K. and Grabke, H. J. (1994) Microstructural characterization and adherence of the α-Al_2O_3 oxide scale on the Fe–Cr–Al and Fe–Cr–Al–Y alloys. *Oxid. Met.* **41,** 343–364.
Whittle, D. P. and Stringer, J. (1980) Improvement in high-temperature oxidation resistance by additions of reactive elements or oxide dispersions. *Phil. Trans. R. Soc. London* **A295,** 309–329.
Yang, W. H. and Srolovitz, D. J. (1994) Surface morphology evolution in stressed solids: Surface diffusion controlled crack initiation. *J. Mech. Phys. Solids* **42,** 1551–1571.